# ANALYSIS OF THE OPERATIONAL PERFORMANCE OF STRAW BALER PICKUP DEVICE BASED ON EDEM AND ADAMS

/

# 基于 EDEM 与 ADAMS 的秸秆打捆机捡拾装置作业性能分析

**Wei-qi CHEN[1)], Yong-cai MA[*1)], Han-Yang WANG[1], Jia-Hao DI[1)], Song Lou[1)]**

[1)] College of Engineering, Heilongjiang Bayi Agricultural University, Daqing/P.R.China

*Tel: +86-459-18745952020; E-mail: myc1631@163.com*

*Corresponding author: Yong-cai MA*

*DOI: https://doi.org/10.35633/inmateh-78-02*

***Keywords***: *pickup device; kinematic simulation; pickup speed ratio; discrete element method; straw collection*

## ABSTRACT

*To improve the utilization rate of rice straw remaining in the field after harvest, a pickup device suitable for collecting rice straw was designed, enabling the secondary utilization of crop residues. A solid model of the pickup device was developed using SolidWorks software, and kinematic simulation analysis of the virtual prototype was performed using ADAMS software. By adjusting the ratio between the pickup device speed and the forward speed of the machine, the motion trajectory of the spring teeth on the pickup roller was modified. The optimal rotational speed range of the pickup roller for achieving the best pickup performance was determined to be 54–137 r/min. A discrete element simulation system was established to model the soil–straw–implement interaction during the pickup operation using Python and EDEM software. Using Design-Expert software, a three-factor, three-level orthogonal experimental design was conducted to determine the optimal combination of operational parameters for the pickup device, including forward speed, pickup roller speed, and ground clearance. Field test results indicated that when the machine forward speed was 4.45 km/h, the pickup roller speed was 90.16 r/min, and the ground clearance was 27.73 mm, the rice straw pickup rate reached 97.22%, indicating that the machine achieved optimal straw pickup performance under these operating conditions.*

## 摘要

*为提高田间收获后水稻农作物秸秆的离田利用率，设计了一种适用于收集水稻秸秆的捡拾装置，实现了农作物废弃秸秆的二次利用。利用 SolidWorks 软件进行捡拾装置的实体建模，在 ADAMS 软件中对虚拟样机进行运动学仿真分析，通过控制捡拾装置转速与机器前进速度的比值改变捡拾滚筒上弹齿的运动轨迹，获得使机器具备最佳捡拾效果的捡拾滚筒转速范围 54~137 r/min。运用 Python 与 EDEM 软件建立土壤-秸秆-机具互相作用的离散元仿真系统进行捡拾作业仿真试验，运用 Design-Expert 软件开展三因素三水平正交组合试验，得到捡拾装置最佳的前进速度、滚筒速度和离地高度等作业参数组合。田间试验结果表明，当机具前进速度为 4.45 km/h，捡拾滚筒转速 90.16 r/min 时，离地高度 27.73 mm 时，水稻秸秆捡拾率为 97.22%，机具在作业时对水稻秸秆的捡拾效果最好。*

## INTRODUCTION

Over the past few centuries, crop harvesting has generated large quantities of straw, making it an important renewable resource *(Zhang et al., 2017)*. However, a significant portion of crop straw is still burned in the fields instead of being properly converted into other forms of energy for utilization *(Ramulu et al., 2023)*. Straw serves as a vital material foundation in agriculture, and its utilization efficiency significantly impacts its application in both agriculture and livestock farming. In response to the national call, open burning and indiscriminate dumping of crop residues should be reduced. This promotes the utilization of crop straw as feed, fuel, and fertilizer, thereby advancing the use of biomass energy and the development of the feed industry *(Cheng., 2023; Huo et al., 2019)*. As one of the key agricultural machines in modern farming, the round baler performs tasks such as straw collection, feeding, and compression, thereby reducing farmers' workload during harvest and enhancing the automation level of straw harvesting. Currently, there are numerous types of straw baling machinery available both domestically and internationally, such as John Deere's F400 series and Krone's Fortima series round balers *(Ruihai et al., 2019)*. The universal baler primarily handles the rolling and bundling of forage and crop residues. The resulting bales feature a tight exterior and loose interior, facilitating ventilation and drying while extending storage duration.

However, the mechanical operations involved in straw collection occur in relatively complex environments, and the operational parameters of baling machinery are difficult to control during field work *(China et al., 2007; Guo et al., 2019)*.

As the first component of the baler to come into contact with forage during operation, the quality of the pickup device performance determines whether the baler achieves optimal results and impacts its overall operational efficiency *(Zhai et al., 2025)*. After conducting relevant operational studies on balers, it was found that significant amounts of straw residue remained on the ground after pickup, indicating incomplete collection. This study takes rice straw as an example, comprehensively considering the agronomic requirements for rice straw collection operations, and analyzes the working process of machinery performing collection and recovery. To improve the operational performance of the baler pickup device and reduce the missed pickup rate, a reasonably dimensioned, easy-to-install roller-type pickup device equipped with spring teeth and without a guard ring was designed. Using SolidWorks computer-aided design software to construct a 3D model of the picking device was developed. Subsequently, ADAMS multibody dynamics simulation software was used to analyze the structural design and operational parameters of each component. This investigation examined the spatial relationships between components and the influence of operational parameters on the missed pickup rate and pickup efficiency. Using EDEM simulation software, a soil-straw-implement model was established to perform discrete element simulation tests on the operational performance of the pickup device. Multiple parameter sets were compared and analyzed with the goal of improving straw pickup efficiency, aiming to identify the optimal working parameter combination and reduce the pickup device's missed pickup rate. Finally, through field trials, the pickup performance of the machinery under optimal operational parameter combinations was validated and analyzed to enhance its pickup efficiency and operational quality.

## MATERIALS AND METHODS

### *Overall structure of the machine and pickup device*

Straw balers primarily pick up and collect scattered rice straw in fields after the autumn harvest, preventing excessive accumulation of abandoned straw. The baler assembly and cross-sectional view are shown in Figure 1. It primarily employs a three-point hitch for connection to front-mounted tractors, with key components including the pickup device, conveyor auger, feed auger, baling mechanism, hydraulic compression device, and knotting device. The picking device primarily consists of multiple spring teeth, a picking roller, a central shaft, guardrails, and other components. Figure 2 shows the overall structure of the pickup roller. The spring teeth are secured to the pickup roller via bolts and washers. In the field of agricultural machinery, spring teeth are an indispensable component of balers, primarily enabling the oscillating motion required for picking up crop stalks. For delicate, soft stalks like rice straw, specially treated metal spring teeth are selected. During machine operation, the spring teeth, driven by the high-speed rotation of the roller, not only pick up and lift the straw but also provide a certain degree of air-assisted conveying for the straw.

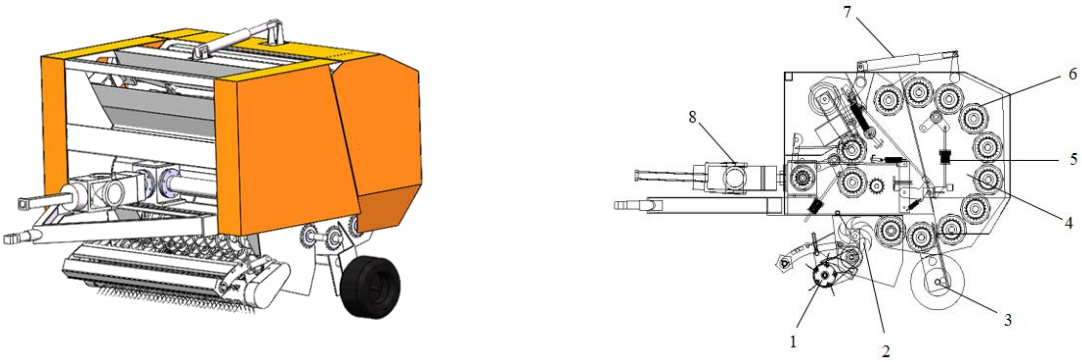


**Fig. 1 - Straw baler overall structure and cross-section diagram**

*1 - pickup device; 2 - feed auger; 3 - land wheel; 4 - baling chamber; 5 - knot-tying device; 6 - compression steel roller; 7 - hydraulic compression device; 8 - universal joint*

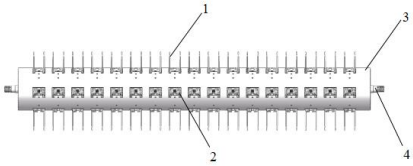


**Fig. 2 - Overall structure of the pickup roller**

*1 - spring tooth; 2 - tooth groove; 3 - pickup roller; 4 - central shaft*

### *Working principle and structural parameters*

During operation, the baler connects the power take-off shaft of the tractor's rear axle to the baler's power input shaft via a universal joint drive shaft. As the tractor pulls the baler forward, the pickup roller rotates at high speed driven by the central shaft, causing the spring teeth mounted on it to move. These spring teeth pick up, lift, and push the rice straw spread across the field, flinging it into the conveyor auger connected to the side panels. The conveyor auger further transports the straw from the edges into the feed auger. Finally, the feed auger conveys the straw into the compression chamber, where hydraulic pressure is applied to form the bale. After the knotter secures the straw bundle, the rear cover automatically opens to discharge the round bale. The resulting round bales can serve as livestock feed for ruminants and also function as biomass fuel for clean energy applications such as power generation, offering significant utilization value.

Based on the cultivation methods of most field crop straws and relevant agricultural machinery design manuals, and comprehensively considering the primary parameters of existing balers and pickup devices, the main structural parameters of the straw baler is shown in Table 1 *(Li., 2003)*.

**Table 1**

**Main structural parameters of the baler and pickup device**

| Structural parameters | Numerical value |
|---|---|
| Overall dimensions [Length×Width×Height/mm] | 4450×2950×2500 |
| Machinery quality [kg] | 5000 |
| Pickup device dimensions [Length×Width×Height/mm] | 2340×950×600 |
| Working width of machinery [mm] | 2200 |
| Supporting power [kW] | ≥125 |

## Kinematics Simulation of a Pickup Device Based on ADAMS

### *Assembly model creation*

To validate the rationality of the device structure and analyze its motion characteristics, the three-dimensional model of the equipment created in SolidWorks was imported into ADAMS multibody dynamics software in x_t format for kinematic simulation. To facilitate the simulation analysis, the model was simplified by hiding components such as the rear section of the implement, retaining only the pickup device section. Boolean operations were performed in ADAMS on the non-moving components outside the pickup device. These components were sequentially merged with the frame according to their contact positions, and interference checks were conducted. All bolts, washers, and spring teeth were constrained to the pickup roller to ensure proper assembly, as shown in Figure 3. The imported 3D model components were then merged, material properties and part colors were defined, gravity was set, and the interface grid was configured. For the drive settings of the machine, a translational drive was applied to the pickup device frame, while both rotational and translational drives were applied to the pickup roller. After these steps, the preliminary configuration of the simulation model was completed *(Liang et al., 2025)*.

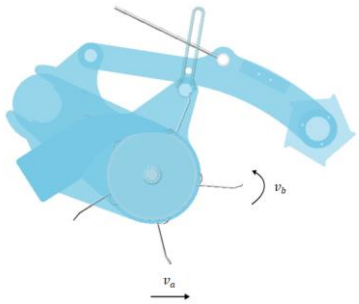

**Fig. 3 - Model of ADAMS picking up device**

### *Theoretical analysis of the movement of the pickup device*

The pickup device is the primary functional component of the implement. During operation, the spring teeth perform both rotational movement around the roller and forward movement in tandem with the implement. Therefore, the absolute motion of the pickup teeth is the combination of the pickup roller's rotation and the machine's forward movement, with its motion trajectory being a cycloid. To clarify the motion trajectory of the spring teeth, the tip point of the spring teeth was defined as the Marker_i point, serving as the observation target for analyzing the motion trajectory. Its theoretical motion trajectory is shown in Figure 4.

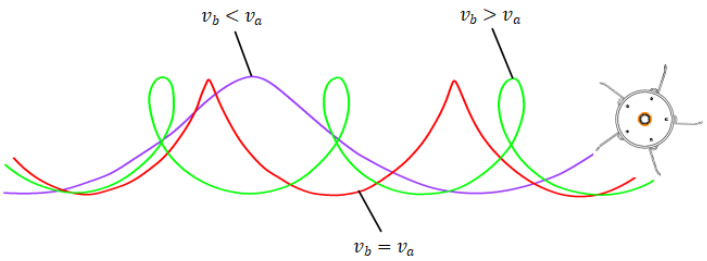


**Fig. 4 - Spring tooth tip motion trajectory under different operating conditions**

To control the motion trajectory of the spring teeth, the forward speed of the implement is defined as $v_a$, and the circumferential linear velocity of the pickup roller is defined as $v_b$, the pickup speed ratio $\lambda$ is expressed as:

$$\lambda = \frac{v_b}{v_a} = \frac{\omega R}{v_a} \tag{1}$$

$$v_b = \frac{n\pi D}{60} = \omega R \tag{2}$$

$$D = 2R$$

Because the trajectory of the spring teeth is related to the pickup speed ratio $\lambda$, the motion trajectory of the spring teeth can be controlled by adjusting this parameter. Therefore, by controlling the pickup speed ratio and analyzing the motion trajectory of the spring teeth, the relationship between the pickup speed ratio and the motion trajectory can be determined *(Wang et al., 2021)*. As shown in Figure 4, when $\lambda < 1$, $v_b < v_a$, the spring teeth cannot effectively perform the pickup function. When $\lambda = 1$, $v_b = v_a$, the motion of the spring teeth is in a transitional state. When $\lambda > 1$, $v_b > v_a$, the trajectories of the spring teeth overlap, forming a ring-shaped cycloidal curve that enables effective pickup. Under the same horizontal displacement, a higher rotational speed results in a greater number of straw stalks being conveyed over the same distance. However, the pickup rate does not increase indefinitely with increasing rotational speed. To ensure normal pickup operation, the circumferential linear speed of the pickup roller should be 1.4–2.4 times the forward speed of the machine *(Yu et al., 2017)*.

***Analysis of spring tooth motion trajectories under different operating parameters***

A single-factor analysis method was employed to conduct kinematic simulations considering the rotational speed of the pickup roller and the forward speed of the machine. Given the characteristics of rice straw being prone to lodging and having high density, and based on literature review and agricultural machinery manuals, it is known that, the forward speed of the baling machine during operation is 3.6~6 km/h *(Li., 2003; Zhang., 2019)*. As determined in the previous section, the value of $\lambda$ must fall between 1.4 and 2.4 for the operation to proceed normally. For convenience in conducting the experiments, the forward speed of the machine was set within the range of 4–6 km/h. Accordingly, the rotational speed of the pickup roller ranged from 54 r/min to 137 r/min. The influence of individual factors on the motion trajectory of the spring tooth tip on the pickup roller was then analyzed using a single-factor approach.

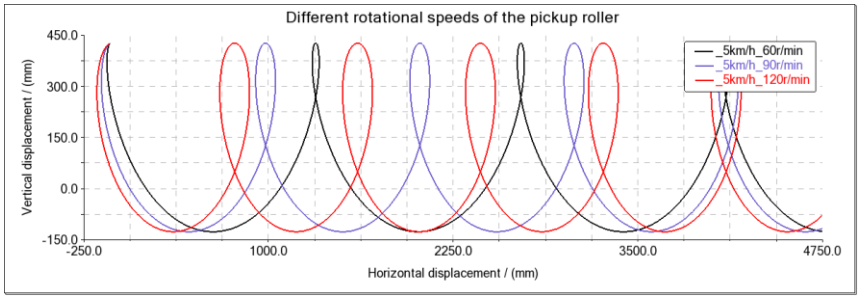


**Fig. 5 - Motion trajectory of spring teeth tips at different pickup roller speeds**

Figure 5 shows the displacement trajectory curves of the spring teeth tips under the single-factor influence of different roller rotational speeds. When the forward speed of the machine is set to 5 km/h, the pickup roller rotational speeds are 60, 90, and 120 r/min. As shown in the figure, the displacement trajectory of the spring tooth tip exhibits a cycloidal pattern.

When the forward speed of the machine remains constant, increasing the rotational speed of the pickup roller causes the ring-shaped cycloidal curve to expand. The higher frequency of the displacement trajectory reduces missed pickup areas and improves straw collection efficiency. However, excessively high pickup roller speeds are not necessarily beneficial for the pickup operation.

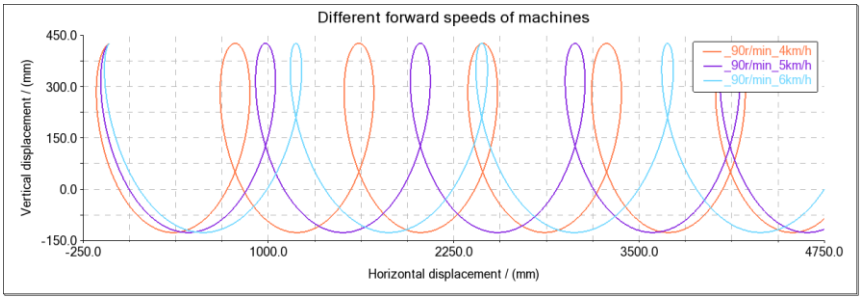


**Fig. 6 - Motion trajectory of spring teeth tips at different forward speeds of the machines**

Figure 6 shows the displacement trajectory curve of the spring teeth tips under the single-factor influence of the overall forward speed of the machine. When the pickup roller speed is set to 90 r/min, the baler's forward speed is set to 4, 5, and 6 km/h, respectively. As shown in the figure, as the forward speed of the machine increases, the ring-shaped cycloidal curve gradually becomes smaller. The frequency of the displacement trajectories decreases, resulting in an increase in missed pickup areas and a reduction in straw pickup efficiency. When the forward speed becomes too high, the ring-shaped cycloidal trajectory may disappear. Therefore, controlling parameters such as the machine forward speed and the pickup roller rotational speed has a significant influence on the pickup efficiency.

## Discrete Element Method-Based Simulation of Pickup Device Operations

### *Establishment of particle models*

EDEM is a virtual simulation software for discrete materials, with its unique simulation technology and excellent performance, it has been widely applied in the design and research of machinery across various agricultural engineering industries *(Barr et al., 2019; Leblicq et al., 2016)*. The accuracy and reliability of discrete element method analysis primarily depend on the suitability of the selected contact model *(Horabik et al., 2016)*. For different analysis subjects, specific contact models must be selected to accommodate varying application scenarios and meet simulation requirements *(Wu et al., 2021)*.

To determine the optimal combination of working parameters for the pickup device and to verify the operational effectiveness of this parameter combination, a discrete element interaction model for soil, straw, and machinery was established using Altair EDEM software. Considering the physical characteristics of rice straw—segmented structure, high flexibility, and hollow geometry—a discrete element particle model of rice straw was developed, as shown in Figure 7. The particle coordinates of the ring-shaped straw model, created using a Python plugin, were imported into the EDEM preprocessing module. A flexible discrete element model of rice straw was then established using the Meta-Particle particle type. Based on field measurements of rice straw, a closed ring structure was constructed by arranging 12 spherical particles with a radius of 0.5 mm in a circular configuration. This ring structure was subsequently extended axially to generate a rice straw particle model with an outer diameter of 5 mm, an inner diameter of 4 mm, and a length of 350 mm.

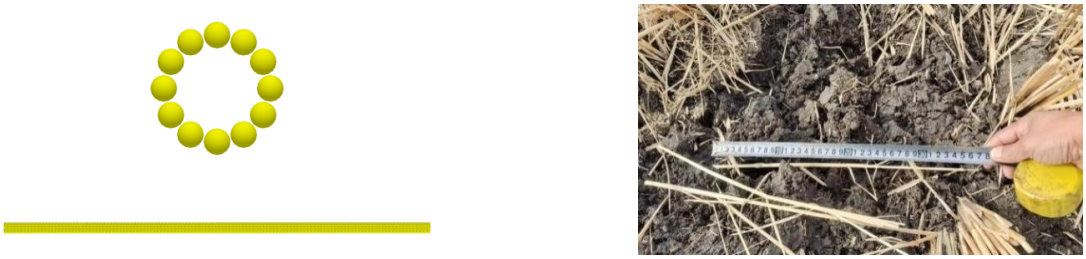

**Fig. 7 - Segmented rice straw pellet model**

To better investigate the interactions among soil, straw, and machinery and to simulate real field operating conditions, a soil–straw–implement interaction model was established. Based on the stratification characteristics of field soil, the thickness of the simulated soil particle layer was set to 100 mm, corresponding to the topsoil layer with similar soil properties *(Dong et al., 2022)*. According to relevant studies, the structural morphology of fertile soil is typically characterized by soil particles that agglomerate into granular and small clod-like aggregates. In discrete element simulations, these aggregates are generally approximated as spherical particles.

However, during the discrete element simulation of soil channel construction, the size of soil particles is constrained by computational limitations and therefore cannot match the actual dimensions of soil particles *(Shi et al., 2017)*. Considering the soil characteristics of the Northeast region, the simulation used soil particles with a radius of 10 mm and a moisture content of 19.26% *(Gou, 2022)*, and a corresponding soil particle model was established. In EDEM software, a soil particle bed model was first created with dimensions of 3000 mm in length, 2500 mm in width, and 500 mm in height. Subsequently, two particle factories were created, and different particle generation times were defined for each factory. Soil particles were first generated to fill the soil trough model. Afterwards, the particle factory position was adjusted to the surface of the soil particle bed, and 12,000 rice straw particles were randomly generated and distributed on the surface. The generated rice straw particles formed a pile with a height of 120 mm, as shown in Figure 8.

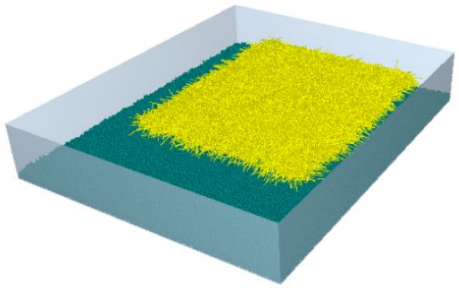

**Fig. 8 - Soil-Straw simulation model**

***Setting of particles contact parameters***

Taking into account the complex interactions between soil particles and their impact on straw pickup, the cohesive interaction between soil particles should employ the Hertz-Mindlin with Bonding V2 contact model. This bonding bond can withstand both tangential and normal stresses. Under external forces, the cohesive force between particles may fracture or break, a phenomenon commonly used in simulating soil particle structures *(Gou., 2022)*. The Hertz-Mindlin with bonding V2 model offers advantages such as simplicity, reliability, and rapid particle modeling. It can also simulate the occasional breakage of straw during the pickup process, making it suitable for the simulation experiments of rice straw pickup in this study *(Xu., 2025)*. The intrinsic parameters and contact parameters of the discrete element simulation models for soil, straw, and machinery can be referenced from relevant literature *(Xu., 2025; Song., 2020; Gou., 2022)*, with specific values shown in Tables 2 and 3. Among these, the bonding parameters—namely the normal contact stiffness, tangential contact stiffness, critical normal stress, and critical tangential stress—can all be obtained through literature review *(Song., 2020)*. The particle bonding radius of rice straw is 1.1 to 1.2 times the particle radius *(Ren., 2023)*. However, the bonding radius of soil particles is related to both moisture content and particle radius.

$$w = \frac{m_2}{m_1 + m_2} = \frac{\rho_2 v_2}{\rho_1 v_1 + \rho_2 v_2} = 19.26\% \tag{3}$$

$$v_1 = \frac{4}{3}\pi R_1^3 \tag{4}$$

$$v_2 = \frac{4}{3}\pi\left(R_2^3 - R_1^3\right) \tag{5}$$

Through formula calculation, the soil particle bonding radius was determined to be 10.97 mm. The bonding parameters are shown in Table 4 *(Shi et al., 2017)*.

**Table 2**

**Intrinsic parameters of simulated materials**

| Material | Parameter name | Numerical value |
|---|---|---|
| soil | Density / (kg·m$^{-1}$) | 1339 |
| | Shear modulus / MPa | $1.25\times10^{6}$ |
| | Poisson ratio | 0.39 |
| straw | Density / (kg·m$^{-1}$) | 227 |
| | Shear modulus / MPa | 1 |
| | Poisson ratio | 0.4 |
| **Material** | **Parameter name** | **Numerical value** |
| steel | Density / (kg·m$^{-1}$) | 7850 |
| | Shear modulus / MPa | $7.9\times10^{4}$ |
| | Poisson ratio | 0.3 |

**Table 3**

**Contact parameters for discrete element simulation models**

| Contact Name | Parameter name | Numerical value |
|---|---|---|
| Soil-Soil | Collision Recovery Coefficient | 0.45 |
| | Static Friction Coefficient | 0.39 |
| | Coefficient of Rolling Friction | 0.21 |
| Soil-Straw | Collision Recovery Coefficient | 0.5 |
| | Static Friction Coefficient | 0.75 |
| | Coefficient of Rolling Friction | 0.05 |
| Soil-Steel | Collision Recovery Coefficient | 0.6 |
| | Static Friction Coefficient | 0.6 |
| | Coefficient of Rolling Friction | 0.05 |
| Straw-Straw | Collision Recovery Coefficient | 0.6 |
| | Static Friction Coefficient | 0.75 |
| | Coefficient of Rolling Friction | 0.01 |
| Straw-Steel | Collision Recovery Coefficient | 0.3 |
| | Static Friction Coefficient | 0.3 |
| | Coefficient of Rolling Friction | 0.01 |

**Table 4**

**Particle bonding parameters**

| Parameter name | Soil | Straw |
|---|---|---|
| Normal contact stiffness / (N·m$^{-1}$) | $3.8\times10^{7}$ | $9\times10^{10}$ |
| Tangential contact stiffness / (N·m$^{-1}$) | $2.4\times10^{7}$ | $9\times10^{6}$ |
| Critical normal stress / Pa | $1.71\times10^{8}$ | $4.29\times10^{10}$ |
| Critical tangential stress / MPa | $7.3\times10^{7}$ | $5.15\times10^{6}$ |
| Particle Bonding Radius / mm | 10.97 | 0.6 |

***Discrete element simulation testing***

After establishing the different particle models, a discrete element simulation system for soil–straw–implement interaction was constructed. The soil–straw simulation model was exported from EDEM software with the export option set to preserve original properties and the simulation start time set to 0 s. As shown in Figure 9, the simplified IGS-format model of the pickup device was imported into the simulation model. Certain components were merged during the configuration process.

The pickup roller was defined as a subordinate component of the frame, ensuring that it followed the frame during motion. Finally, the positional parameters of the pickup device components were configured so that the device was positioned directly above the soil trough model for simulation testing.

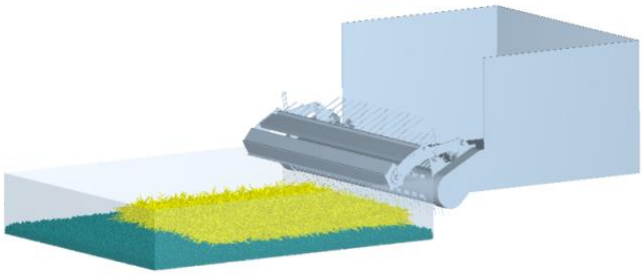

**Fig. 9 - Soil-Straw-Machinery simulation operation model**

During the straw pickup operation simulation, the pickup roller speed, machine forward speed, and spring tooth ground clearance were selected as independent variables, while the straw pickup rate was used as the response variable. By comparing the simulation results, the parameter combination that produced the best pickup performance—i.e., the highest pickup rate—was identified for each set of operational conditions in the discrete element simulation tests. To simplify the implement model and facilitate analysis of the pickup process, a collection container was added behind the pickup device, as the implement continuously gathers straw during operation. This configuration allows the straw pickup rate to be calculated after the implement completes the collection of all straw particles.

To further investigate the straw pickup efficiency, the area where the machine passed over and picked up rice straw was selected in the EDEM software post-processing. The straw pickup rate p was calculated based on the ratio of the weight of missed straw to the weight of picked-up straw.

$$p = \frac{m}{M+m} \times 100\% \tag{6}$$

According to reference materials, the forward operating speed of agricultural machinery ranges from 4 to 6 km/h. The working height of the spring teeth above ground is 20 to 55 mm. The rotational speed range of the pickup device roller is determined to be 60 to 120 r/min.

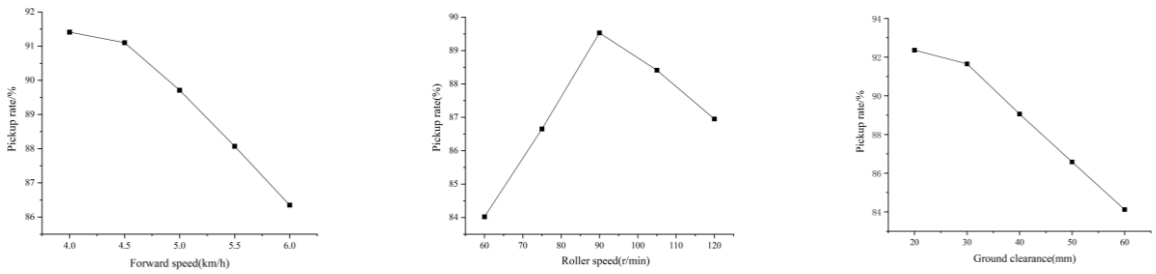


(a) (b) (c)

**Fig. 10 - Effects of experimental factors on straw pickup rate**

An analysis was conducted on the effects of various experimental factors on the pickup rate during straw collection. As shown in Figure 10 (a), the pickup rate gradually decreased with increasing forward speed. A speed of 4.5 km/h was selected as the zero level for the response surface experiment. In Figure 10 (b), the pickup rate first increases and then decreases as the roller speed rises. A speed of 90 r/min is selected as the zero level for the response surface experiment. Figure 10 (c) shows that the pickup rate gradually decreases as the operating height of the device increases. A height of 30 mm was selected as the zero level for the response surface experiment.

***Simulation results and analysis***

By adjusting various operational parameters of the pickup device—specifically machine forward speed, pickup roller rotational speed, and spring teeth ground clearance height as experimental factors—and using straw pickup rate as the evaluation metric, a three-factor, three-level orthogonal combination test employing the Box-Behnken Design was conducted using Design-Expert data analysis software. This analysis examined the impact of different parameter combinations on rice straw pickup efficiency. The factor level coding table and experimental design are shown in Tables 5 and 6.

**Table 5**

**Trial factor level coding table**

| Experimental level | Experimental factors | | |
|---|---|---|---|
| | Forward speed A / ($km \cdot h^{-1}$) | Roller speed B / (r/min) | Ground clearance C / (mm) |
| -1 | 4 | 75 | 20 |
| 0 | 4.5 | 90 | 30 |
| 1 | 5 | 105 | 40 |

**Table 6**

**Response surface experiment results**

| Serial number | Test parameters | | | Evaluation indicators |
|---|---|---|---|---|
| | A | B | C | pickup rate / % |
| 1 | 4 | 75 | 30 | 90.77 |
| 2 | 5 | 75 | 30 | 89.53 |
| 3 | 4 | 105 | 30 | 92.11 |
| 4 | 5 | 105 | 30 | 91.58 |
| 5 | 4 | 90 | 20 | 93.53 |
| 6 | 5 | 90 | 20 | 92.50 |
| 7 | 4 | 90 | 40 | 90.04 |
| 8 | 5 | 90 | 40 | 89.16 |
| 9 | 4.5 | 75 | 20 | 89.69 |
| 10 | 4.5 | 105 | 20 | 92.82 |
| 11 | 4.5 | 75 | 40 | 87.72 |
| 12 | 4.5 | 105 | 40 | 87.95 |
| 13 | 4.5 | 90 | 30 | 98.02 |
| 14 | 4.5 | 90 | 30 | 97.52 |
| 15 | 4.5 | 90 | 30 | 97.74 |
| 16 | 4.5 | 90 | 30 | 97.62 |
| 17 | 4.5 | 90 | 30 | 97.85 |

Multiple regression analysis of the experimental data resulted in a quadratic polynomial regression model, and the regression equation is expressed as follows:

$$Y=97.75-0.46A+0.8438B-1.71C+0.1775AB+0.0375AC - 0.7250BC-2.5A^2-4.26B^2-3.95C^2 \quad (7)$$

The analysis results are shown in Table 7. The regression model exhibits high significance, high fitting accuracy, and good correlation. By comparing the p-values of various parameters in the model. Among the interaction terms, the interaction AC between forward speed and ground clearance height had the least effect on pickup rate. Next was the interaction AB between forward speed and roller rotational speed. The interaction BC between roller rotational speed and ground clearance had the most significant effect on pickup rate.

Table 7

**Results straw pickup rate regression model variance analysis**

| Sources of variance | Sum of Squares | Degrees of freedom | Mean Square | F | P |
|---|---|---|---|---|---|
| model | 219.66 | 9 | 24.41 | 1099.56 | < 0.0001 |
| A | 1.69 | 1 | 1.69 | 76.26 | < 0.0001 |
| B | 5.70 | 1 | 5.70 | 256.59 | < 0.0001 |
| C | 23.36 | 1 | 23.36 | 1052.36 | < 0.0001 |
| AB | 0.1260 | 1 | 0.1260 | 5.68 | 0.0487 |
| AC | 0.0056 | 1 | 0.0056 | 0.2534 | 0.6301 |
| BC | 2.10 | 1 | 2.10 | 94.72 | < 0.0001 |
| A2 | 26.21 | 1 | 26.21 | 1180.85 | < 0.0001 |
| B2 | 76.32 | 1 | 76.32 | 3438.45 | < 0.0001 |
| C2 | 65.61 | 1 | 65.61 | 2955.95 | < 0.0001 |
| residual | 0.1554 | 7 | 0.0222 | | |
| lack of fit | 0.0026 | 3 | 0.0009 | 0.0225 | 0.9947 |
| pure error | 0.1528 | 4 | 0.0382 | | |

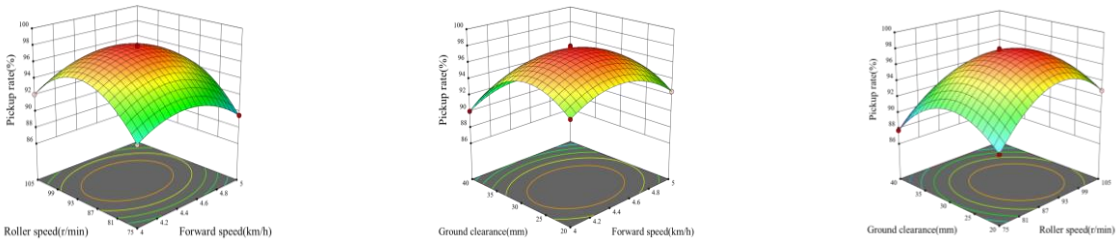


(a) (b) (c)

**Fig. 11 - Interaction effect response surface plot**

Figure 11 (a) shows the effect of the interaction between forward speed and roller rotational speed on straw pickup rate. When roller rotational speed and ground clearance are constant, the straw pickup rate gradually decreases as the forward speed of the implement increases. This occurs because the increased forward speed reduces the number of contacts between the pickup spring teeth and the straw, leading to more straw being missed and thus a decrease in the pickup rate.

As shown in Figure 11 (b), when the forward speed of the implement and the roller rotational speed remain constant, the straw pickup rate gradually decreases as the ground clearance increases. This occurs because as the pickup device rises higher off the ground, the penetration depth of the spring teeth into the straw decreases. Straw lying close to the surface cannot be picked up, leading to a gradual reduction in the pickup rate. Ground clearance directly affects the straw pickup rate.

As shown in Figure 11(c), when the ground clearance and forward speed remain constant, the straw pickup rate first increases and then gradually decreases as the rotational speed of the pickup roller increases. This occurs because the pickup speed ratio between the forward speed and the roller speed changes with increasing roller speed. Initially, the increase in roller speed raises the number of contacts between the spring teeth and the straw, thereby improving the pickup rate. However, when the roller speed becomes excessively high, the kinetic energy of the spring teeth during collision with the straw increases significantly. As a result, the straw is easily thrown away by the high-speed rotating spring teeth and may be ejected from the pickup zone, which consequently reduces the straw pickup rate.

## RESULTS

### *Field validation protocols and trials*

For the straw pickup rate regression model, the optimization function in Design-Expert software was employed to solve the regression model. The optimal parameter combination obtained was a forward speed of 4.45 km/h, a roller speed of 91.16 r/min, and a ground clearance of 27.73 mm. At these settings, the straw pickup rate reached 98.014%.

The pickup device was manufactured based on the optimal combination of operational parameters. Field trials were conducted according to rice baling agronomic requirements to verify whether the device meets operational demands. The trial process is illustrated in Figure 12.

**Fig. 12 - The process of field trial**

Through conducting five sets of optimal parameter pickup trials on rice straw within a specified range after field harvesting, measurements and calculations were performed on the quality of collected bales and residual rice straw on the ground. The test data are shown in Table 8. The results indicate that the average straw pickup rate was 97.22%, differing by 0.794% from the simulation result of 98.014%. Under optimal operating parameters, the baler's pickup device meets agronomic requirements for rice straw baling and delivers the best pickup performance.

**Table 8**

**Field trial results**

| Serial Number | Forming and Bundling Quality / kg | Quality of missed straw / kg | Pickup rate / % |
|---|---|---|---|
| 1 | 198.61 | 6.02 | 97.06 |
| 2 | 199.08 | 5.88 | 97.13 |
| 3 | 200.42 | 4.49 | 97.81 |
| 4 | 197.27 | 6.59 | 96.77 |
| 5 | 199.24 | 5.43 | 97.35 |
| Mean value | 198.92 | 5.68 | 97.22 |

## CONCLUSIONS

(1) Motion simulations were performed in ADAMS software at different pickup roller rotational speeds, with the straw baler forward speed set to 5 km/h. The motion trajectory of point Marker_i, located at the tip of the spring tooth, was obtained. The analysis shows that when the pickup speed ratio $\lambda > 1$, the spring teeth can effectively perform the pickup function. The pickup device operates normally when the pickup roller rotational speed ranges from 54 to 137 r/min.

(2) A soil–straw–implement interaction model was established using Python programming and EDEM discrete element simulation software. A response surface experiment based on the Box–Behnken design was conducted with the following factors: machine forward speed, pickup roller rotational speed, and spring tooth ground clearance. The straw pickup rate was used as the evaluation index. The Design-Expert analysis results indicate that the optimal operating parameter combination for the straw baler pickup device is a machine forward speed of 4.45 km/h, a pickup roller rotational speed of 90.16 r/min, and a ground clearance of 27.73 mm. Under these conditions, the predicted straw pickup rate is 98.014%. This optimal parameter combination can serve as a reference for parameter settings in subsequent field trials and machinery design.

(3) Field validation tests measured a straw pickup rate of 97.22%, which differs from the simulation result by 0.794%. This small deviation indicates that the simulation results are reliable and that the pickup device meets the agronomic requirements for the collection and baling of rice straw.

## ACKNOWLEDGEMENT

This work was supported by Heilongjiang Provincial Key R&D Program (2024ZXDXB45) and Double First-Class Discipline Collaborative Innovation Achievement Construction Project (LJGXCG2022-107).

## REFERENCES


[1] Barr, J., Desbiolles, J., Fielke, J., Ucgul, M. (2019). Development and field evaluation of a high-speed no–till seeding system [J]. *Soil and Tillage Research*, Vol194: 104337.

[2] Cheng, J. (2021). The Impact of Straw Returning to Fields on Ecological and Environmental Resources in Farmland [J] *Environmental Engineering* Vol.29, No.39, pp. 318.

[3] China Academy of Agricultural Mechanization Sciences. (2007). Agricultural Machinery Design Manual [M]. *Beijing: Agricultural Science and Technology Press*.

[4] Dong, X.Q., Su, C., Zheng, H.N., et al. (2022). Analysis of Soil Disturbance Processes During Vibratory Deep Tillage Based on the DEM-MBD Coupling Algorithm [J]. *Journal of Agricultural Engineering*, Vol.38, No.1, pp. 34-43.

[5] Gou, J.B. (2022). Design and Testing of an Involute Side-Deep Fertilizer Furrow Opener for No-Till Seeders [D]. *Northeast Agricultural University*.

[6] Huo, L.L., Zhao, L.X., Meng, H.B., et al. (2019). Research on the Comprehensive Utilization Potential of Crop Straw in China [J]. *Journal of Agricultural Engineering*, Vol.35, No.13, pp. 218-224.

[7] He, Z.Q., Guo, Z.P., Li, R.P., et al. (2019). Research on Parameter Optimization of the Pickup Device for the 9YG-1.2 Round Baler [J]. *Feed Industry*, Vol.40, No.15, pp. 9-15.

[8] Horabik, J., Molenda, M. (2016). Parameters and contact models for DEM simulations of agricultural granular materials: A review[J]. *Biosystems Engineering*, Vol.147, pp. 206-225.

[9] Li, B.F. (2003). Agricultural Machinery [M]. *Beijing: China Agriculture Publishing House*.

[10] Liang, J., Zhu, H.J., Guo, W., et al. (2025). Design of a Disc-Type Seedling Transplanter End Effector Based on EDEM-ADAMS Coupled Simulation [J]. *Agricultural Mechanization Research*, Vol.47, No.12, pp. 10-19.

[11] Leblicq, T., Smeets, B., Ramon, H., Saeys, W. (2016). A discrete element approach for modelling the compression of crop stems [J]. *Computers and Electronics in Agriculture*, Vol.123, pp. 80-88.

[12] Ruihai Agricultural and Animal Husbandry Equipment. (2019). Krone's New Generation BiGX Silage Harvesting Machinery [J]. *Agricultural Machinery*, No.4, pp. 115.

[13] Ren, Z.D. (2023). Design of Comb-Type Castor Bean Harvesting Device and Study on the Mechanism of Capsule Damage [D]. *Shenyang Agricultural University*.

[14] Ramulu, C., Pateriya, R.N., Naik, M.A. *et al.* (2023). A residue management machine for chopping paddy residues in combine harvested paddy field. *Scientific Reports* Vol.13, pp. 5077.

[15] Shi, L.R., Zhao, W.Y., Sun, W. (2017). A Discrete Element-Based Soil Particle Contact Model for Farmland in Arid Northwest China and Parameter Calibration [J]. *Journal of Agricultural Engineering*, Vol.33, No.21, pp. 181-187.

[16] Song, W.B. (2020). Research on Straw-Incorporated Soil Tillage Simulation and Energy Consumption Management Based on the Discrete Element Method [D]. *Nanjing Agricultural University*.

[17] Wang, Q.Q., Jiang, Y.C., Li, L.H., et al. (2021). Performance analysis of a spring-tooth roller pickup of straw baler via coupling simulation[J]. *International Journal of Agricultural and Biological Engineering*, Vol.14, No.3, pp. 159-165.

[18] Wu, Z., Wang, X., Liu, D, Xie, F, Ashwehmbom, L., Zhang, Z., Tang, Q. (2021). Calibration of discrete element parameters and experimental verification for modelling subsurface soils [J]. *Biosystems Engineering*, Vol.212, pp. 215-227.

[19] Xu, G.Q. (2025). Design and Testing of a Rice Combine Harvester Straw Chopping Device [D]. *Shenyang Agricultural University*.

[20] Yu, Z.H., Mo, R. G. B. L. G., Wang, W.M., et al. (2017). Comparative Performance Study of Toothed Roller-Type Hay Pickup Machines [J]. *Agricultural Mechanization Research*, Vol.39, No.2, pp. 122-127.

[21] Zhang, F.S., (2019). Design Simulation and Experimental Study of a Toothed Roller Pickup Device [D]. *Northeast Agricultural University*.

[22] Zhai, G.X., Gao, X.H., Wang, Z.H., et al. (2025). Design and Testing of a Large High-Density Square Bale Baler [J]. *Journal of Agricultural Machinery*, Vol.56, No.11, pp. 9-15.

[23] Zhang, Z. et al. (2017). Global overview of research and development of crop residue management machinery. *Applied Engineering Agriculture* Vol.33, No.3 pp. 329–344.